Pectin Remodeling and Involvement of AtPME3 in the Parasitic Plant-Plant Interaction *Arabidospis thaliana* – *Phelipanche ramosa*

Cyril Grandjean , Christophe Veronesi , Christine Rusterucci , Charlotte Gautier , Yanis Maillot , Maïté Leschevin , Françoise Fournet , Jan Drouaud , Paulo Marcelo , Luciane Zabijak , Philippe Delavault , Philippe Simier , Sophie Bouton * , Karine Pageau *

Posted Date: 16 July 2024

doi: 10.20944/preprints202407.1259.v1

Keywords: cell wall; pectin acetyl esterase; pectin methyl esterase; Pectin Remodeling Enzymes; *Phelipanche ramosa-Arabidopsis thaliana*

Article

Pectin Remodeling and Involvement of AtPME3 in the Parasitic Plant-Plant Interaction *Arabidospis thaliana–Phelipanche ramosa*

Cyril Grandjean [1,†], Christophe Veronesi [2,†], Christine Rusterucci [1], Charlotte Gautier [1], Yanis Maillot [1], Maïté Leschevin [1], Françoise Fournet [1], Jan Drouaud [3], Paulo Marcelo [4], Luciane Zabijak [4], Philippe Delavault [2], Philippe Simier [2], Sophie Bouton [1,*,‡] and Karine Pageau [1,*,‡]

[1] UMR INRAE 1158 BioEcoAgro, BIOlogie des Plantes et Innovation, Université de Picardie Jules Verne, Amiens, France; cyril.grandjan@u-paris.fr (C.G.); christine.rusterucci@u-picardie.fr (C.R.); charlotte.gautier@u-picardie.fr (C.G.); yanis.maillot@u-picardie.fr (Y.M.); maite.leschevin@u-picardie.fr (M.L.); francoise.fournet@u-picardie.fr (F.F.)

[2] Equipe Rhizoplante: Interactions plantes-plantes et signaux rhizosphériques, Unité en Sciences Biologiques et Biotechnologies (US2B), UMR CNRS 6286 - UFR des Sciences, 2 rue de la Houssinière F-44322 Nantes cedex 03, France; christophe.veronesi@univ-nantes.fr (C.V.); philippe.delavault@univ-nantes.fr (P.D.); philippe.simier@univ-nantes.fr (P.S.)

[3] Centre Régional de Ressources en Biologie Moléculaire UPJV, Bâtiment Serres-Transfert Rue Dallery - UFR des Sciences, Passage du sourire d'Avril, F-80039, Amiens, France; jan.drouaud@inrae.fr (J.D.)

[4] Plateforme d'Ingénierie Cellulaire & Analyses des Protéines ICAP Université de Picardie Jules Verne, Amiens, France; paulo.marcelo@u-picardie.fr (P.M.); luciane.zabijak@u-picardie.fr (L.Z.)

* Correspondence: sophie.bouton@u-picardie.fr (S.B.); karine.pageau@u-picardie.fr (K.P.)

† These authors contributed equally to this work.

‡ These authors also contributed equally to this work.

Abstract: *Phelipanche ramosa* is a root parasitic plant fully dependent on host plants for nutrition and development. Once germinated, the parasitic seedling develops inside of the infected roots a specific organ, the haustorium, thanks to notably cell wall degrading enzymes of haustorial intrusive cells and induced modifications in host's cell walls. The model plant *Arabidopsis thaliana* is susceptible to *P. ramosa*, thus mutants in cell wall metabolism, notably in pectin remodeling like *Atpme3-1*, are of interest in studying the involvement of cell wall degrading host's enzymes in establishment of the plant-plant interaction. Host-parasite co-cultures in mini-rhizotrons systems revealed that parasite attachments are twice more numerous and tubercle growth is quicker on *Atpme3-1* roots than on WT roots. When compared to the WT, increase in susceptibility in the mutant is associated to reduction in PME activity in roots and to lowering in the degree of pectin methylation at the host-parasite interface, as detected immunohistochemically in infected roots. In addition, both WT and *Atpme3-1* responded to infestation by modulations in expression of PAE and PME encoding genes and in global related enzymes activities in roots, before and after parasite attachment. However, modulations differ in WT and *Atpme3-1* and this may contribute to different pectin remodeling in roots and contrasted susceptibility to *P. ramosa*. By this integrative study, we could define a model of the cell wall response to this particular biotic stress and indicate for the first time the role of PME3 in this parasitic plant-plant interaction.

Keywords: cell wall; pectin acetyl esterase; pectin methyl esterase; pectin remodeling enzymes; *Phelipanche ramosa-Arabidopsis thaliana*

 doi:10.20944/preprints202407.1259.v1

1. Introduction

Among *Orobanchaceae* plants, the branched broomrape, *Phelipanche ramosa* L. Pomel, is an obligate parasitic plant, with a weedy life in cropping areas. Its expansion is not controlled to date and so it is an important pest in Solanaceae (tomato, tabacco), Brassicaceae (cabbage, rapeseed) and Cucurbitaceae fields, especially in central Europe [1,2].

Once germination achieved thanks to eliciting molecules exudated from host roots, mostly strigolactones, the primary root tip differentiates into a specialized organ called haustorium, also in response to host-derived phytohormones (cytokinins) for the establishment of physical and physiological interactions with the host plant [3,4]. In a compatible interaction, the haustorial intrusive cells (HICs) invade the host root cortex, reach the stele, and successfully connect to xylem and phloem tissues similarly to graft junctions. Water and nutrient spoliation from the host results in haustorium growth, distending host root tissues and becoming outside the host root a storage organ, the tubercle. A floral meristem develops into a subterranean shoot, emerges above the soil, branches and blooms. Self-pollinization triggers the production of several thousand seeds that can remain viable in the soil for more than twenty years, resulting in severe soil pollution [5].

A number of studies have investigated the dynamics of the plant cell wall in response to abiotic and biotic stresses [6]. Plant cell wall is a complex structure composed of cellulose microfibrils and non-cellulosic neutral polysaccharides embedded in a physiologically active pectin matrix, cross-linking with structural proteins and lignin, depending on the tissue or organ [7,8]. The primary cell wall of growing cells is distinctive from the secondary cell wall that is deposited within the primary wall of specific cell types with specialized functions. In addition, the middle lamella, a pectin layer, fills the space between the adjacent cells and firmly adheres to them [9]. In the context of plant parasitism, the cell-wall degrading enzymes of the HICs modify the adjacent host cell wall [10,11]. Many studies in *Orobanchaceae* focused on Pectin Remodeling Enzymes (PREs: pectin acetyl esterase, PAE; pectin methylesterase, PME); polygalacturonases, PG; pectate lyases, PL) [11–16]. They act in concert to weaken the host cell wall, then facilitating the progression of the HICs into the infested roots. Immunolabeling experiments revealed the presence of highly de-esterified pectin in host cell walls correlated with the presence of PME and high pectinolytic activity in HICs and adjacent apoplast [17,18]. Accordingly, high pectinolytic activities from the infecting parasite correlate with high aggressiveness against the host plant [13].

The alteration of the cell wall integrity in infected plants is a signal activating effective defensive responses [19]. Cell wall fragments such as oligogalacturonides (OGs) induce the basal plant defenses [20]. OGs correspond to oligomers of galacturonic acids released from homogalacturonan, a major cell wall pectin component [21,22]. Their recognition through Wall Associated Kinases (WAKs, [23]), membrane-localized receptors, is considered as a system for monitoring pectin integrity that induces a set of defense responses, such as the accumulation of reactive oxygen species (ROS) and Pathogenesis Related Proteins [20,24]. Interestingly, a cell-wall kinase over-expressed early in tomato roots challenged to *P. ramosa* [25], acting likely as a sensor of cell wall alterations during broomrape attack.

Among the PME isoforms in Arabidopsis, PME3 triggers the susceptibility to necrotrophic fungal pathogens and parasitic nematodes [26,27]. The responsiveness to OGs through the activation of WAKs receptors increases in the *Atpme3-1* mutant. Accordingly, the mutant exhibits low PME activity and high degree of HG methyl esterification in roots and hypocotyls in comparison to the WT [23,28]. As reported by Pérez-De-Luque et al. (2006) in the incompatible interaction *Vicia sativa* - *Orobanche crenata*, the production of a mucilage rich in de-esterified pectin in xylem vessels of the attacked plants triggers the incompatibility by obstructing xylem vessels and then preventing the development of the attached parasite. Altogether, the studies carried out to date suggest that pectin and PREs play also a major role in the parasitic plant-plant interactions, notably by conditioning both the haustorium development and the activation of defense mechanisms in the infected roots.

In the presents study, we develop an integrative approach in WT and *Atpem3-1* mutant to capture the modifications of pectin in *A. thaliana* challenged to the parasitic plant *P. ramosa* and to address the question of the involvement of AtPME3 in this parasitic plant-plant interaction.

 doi:10.20944/preprints202407.1259.v1

2. Results

2.1. P. ramosa Has Significantly Fewer Putative PREs Encoding Genes than A. thaliana

In several plant species, PREs belong to large multigenic families [30]. In Arabidopsis, 243 PREs were counted and divided into 12 PAE, 66 PME, 71 PMEi, 26 PL and 68 PG ([22]; cellwall.genomics.purdue.edu, accessed on 10 May, 2021) (Figure 1). According to InterProScan software (https://www.ebi.ac.uk/InterProScan, accessed on 11 May, 2021), UniProt sequence data (https//www.uniprot.org, accessed on 15 May, 2021), and the PREs gene sequences obtained by *de novo* transcriptome assembly [3], PREs were globally twice less abundant (128) in *P. ramosa* than in *A. thaliana* (243), independently of the PREs tested, except for PAE family. Fourteen PAEs were accounted in the parasite against 12 PAE in Arabidopsis. Moreover, the PREs number in *P. ramosa* was closer to that in commelinid monocotyledons [22], which had a cell wall of type II with a significant reduction of pectins and xyloglucans in comparison with the Arabidopsis type I cell wall [31], https//www.uniprot.org, accessed on 15 May, 2021).

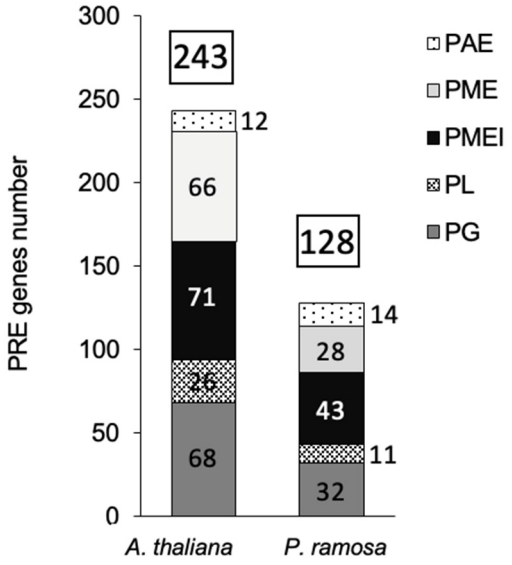

Figure 1. *PREs* putative genes number in *A. thaliana* and P. *ramosa*.

PREs families, associated with a specific Pfam domain (PME: PF1095, PMEi: PF04043, PAE:PF03283, PG: PF00295, PL:PF00544, https//www.uniprot.org) were counted according to InterProScan software (https://www.ebi.ac.uk/InterProScan), UniProt sequence data (https//www.uniprot.org) and PREs gene sequences obtained by de novo transcriptome assembly (Goyet et al., 2019).

2.2. Atpme3-1 Is More Susceptible to P. ramosa than WT

No parasite attachment was detected at 6 hai, 12 hai and 8 dai. The first attachments to WT and *Atpme3-1* occurred during the second week following infestation, with the finding at 14 dai that the parasite attachments (stages 1 and 2) were significantly more numerous on At*pme3-1* (Median: 11.5) than on WT (Median: 4) (Figures 2). Very fewer tubercles reached the stage 3 at this early time point of infestation (Figure 2C). Later, at 28 dai, the total number of parasite attachments counted double on both WT and *Atpme3-1* and most reached the stages 2 and 3. They were still more numerous on *Atpme3-1* (Median: 40) than on WT (Median: 26). During the two following weeks, the total number of parasite attachments did not change significantly, thus marking the maximum level of infestation at 28 dai for WT and *Atpme3-1*. However, parasite continued to develop, and faster on *Atpme3-1*. At 42 dai, there were no more stage 1-attachments to WT and *Atpme3-1*, the number of stage 2-attachments decreased while the number of tubercles at the stage 3 increased, and more obviously on *Atpme3-1*.

 doi:10.20944/preprints202407.1259.v1

2.3. Atpme3-1 Displays Lower HG Methyesterification Degree than WS at the Host-Parasite Interface

Immunolabelling experiments from young control and infected lateral roots was carried out to clarify the HG distribution patterns *in* WT and *Atpme3-1*, especially at the host-parasite interface during haustorium development (stage 1-attachments, at 14 dai) when pectin remodeling could be very intensive in the host roots due to haustorium-secreted cell-wall-modifying enzymes [15,32].

In control conditions, immunolabelling with LM20 antibody resulted in a significant signal (green) in the conductive xylem vessels in both WT and *Atpme3-1* roots (Figure 3A,B), revealing highly methylesterified HGs, while no labelling was detected using LM19 antibody (Figure 3C,D).

In infected WT, weak LM19 and strong LM20 signals were detected at the host-parasite interface (Figure 3G,E). In contrast, both LM19 and LM20 signals were low in infected *Atpme3-1*, showing lower HG methylesterification levels at the host-parasite interface in *Atpme3-1* than in WT.

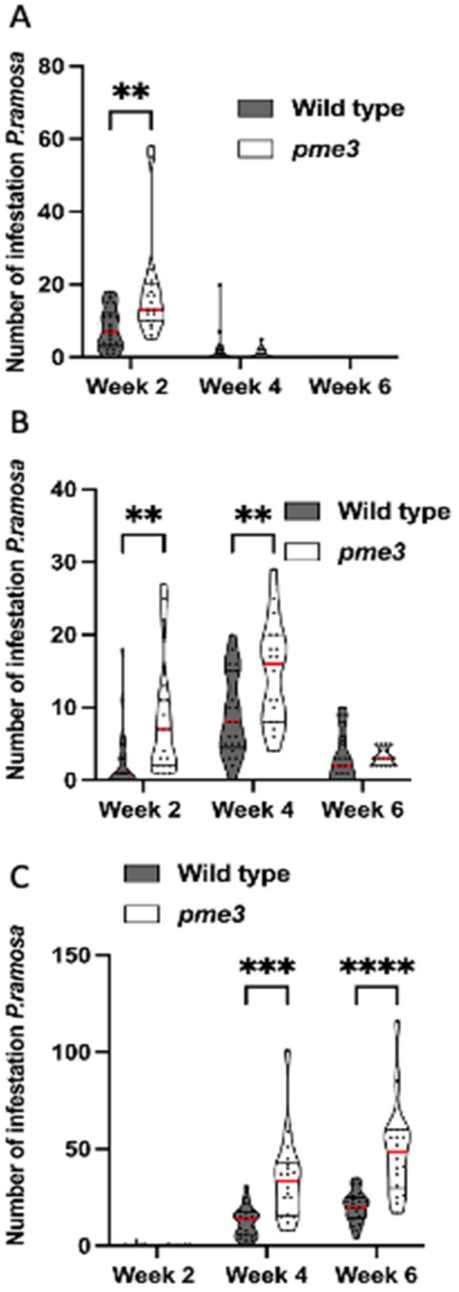

Figure 2. Number of *P. ramosa* attachments on roots of WT or Atpme3-1 along different developmental stage (truncated violin plot). (A) Stage 1, (B) Stage 2, (C) Stage 3 or growing tubercle. Red line represents the median, black line the quartiles, black dot represents biological replicate (n ≥ 3

 doi:10.20944/preprints202407.1259.v1

biological replicates per genotype). **, P < 0.01, ***, P < 0.001, ***, P < 0.0001, multiple T-Test (FDR correction 0.1%).

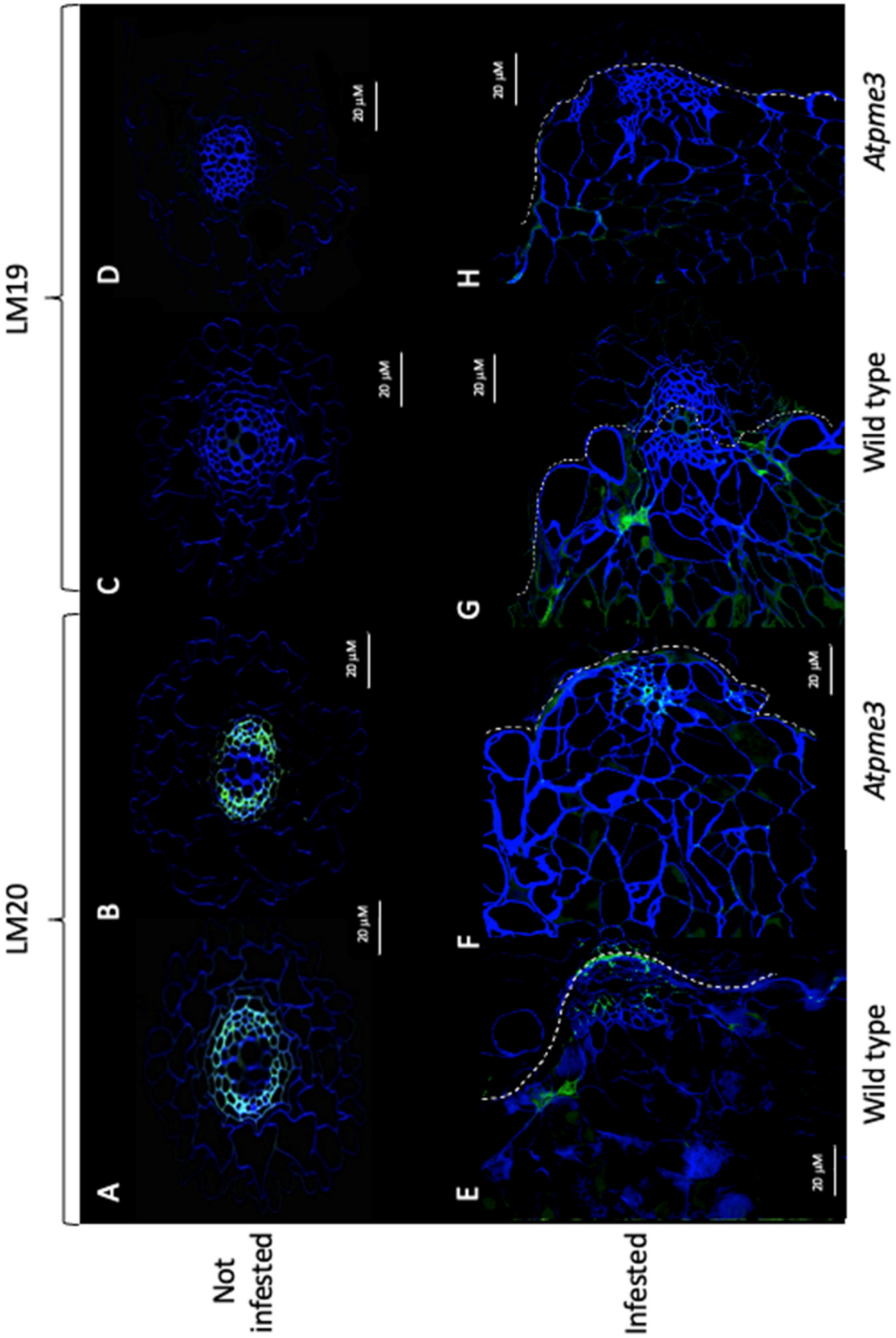

Figure 3. Distribution patterns of homogalacturonans (HG) at the host-parasite parasitic interface. Parasite corresponds to the early stage 1 at 14 dai. Sections of control WT and Atpme3-1: A, C and B,

 doi:10.20944/preprints202407.1259.v1

D, respectively. Sections of infected roots of WT and Atpme3-1: E, G and F, H, respectively. Sections were labelled with LM19 (C, D, G and H) and LM20 (A, B, E and F) antibodies recognizing low and high methylesterified HG, respectively. Calcofluor White, which stains both cellulose and other B-1,4-glycans, was used to visualize cell walls. Bars = 20 μm.

2.4. The Infestation Modulates the Expression of PREs Genes in a Different Way in WT and Atpme3-1 Both before and after Parasite Attachment

PRE gene expression in the host roots under control and infestation conditons was assessed, by using primers specific to Arabidopsis sequences (Table S1).

Among the 12 PAE encoding genes in Arabidopsis, only *PAE7* presented a strong expression, which was 1000 times higher in comparison with the other *PAE* genes (Table S2). In control conditions, WT and *Atpme3-1* displayed similar levels in *PAE7* expression only at the early time point corresponding to 6 hai, the levels becoming much lower in the mutant at the time points corresponding to 12 hai and 14 dai. *PAE7* expression was modulated by infestation in WT and *Atpme3-1* roots in a different way, thus dropping at 6 hai and 12 hai in WT but only at 6 hai in *Atpme3-1*. Later, modulation in the mutant consisted in *PAE7* over-expression at 6 hai and 14 dai, while decreasing and unchanged levels were observed in infested WT at 6 hai and 14 dai, respectively. Finally, WT displayed higher level in *PAE7* expression than *Atpme3-1* at 14 dai in both control and infestation conditions (Figure 4A,B and C-PAE).

Among the 66 genes members of the PME family in Arabidopsis, only 8 genes were highly expressed at 6 hai in WT and *Atpme3-1*. *PME18* and *PME31* were systematically the most expressed genes (Figure 4-PME-WT et 5-PME-*Atpme3-1*). Five expressed genes were common to the two genotypes: *PME17, PME18, PME31, PME35* and *PME51*. *PME40* and *PME62* expressed especially in WT whereas *PME41* expressed only in *Atpme3-1*.

Comparatively, a small number of *PME* genes were highly expressed in both genotypes at 12 hai, and included *PME18, PME17, PME31, PME35* and *PME51* in WT and only *PME18* and *PME62* in *Atpme3-1* (Figure 4, B-PME-WT and B-PME-*Atpme3-1*). Expression of all these genes also decreased at this time point in response to infestation (Figure 4, B-PME WT), except *PME 18* expression that strongly increased in *Atpme3-1* (Figure 4, B-PME *Atpme3-1*).

The expression of several *PME* genes, especially *PME 40*, enhanced at 14 dai in infected WT (Figure 4, C-PME WT). Then *PME40*, in addition to *PME18* and *PME31*, became the most expressed *PME* genes in infected WT. A similar feature was observed in infected *Atpme3-1*, particularly for *PME62* and *PME31* (Figure 4, C-PME Atpme3-1).

More generally, the expression of certain *PME* genes increased in response to infestation in both genotypes, but this was observed much earlier, as soon as 12 hai, in *Atpme3-1*.

 doi:10.20944/preprints202407.1259.v1

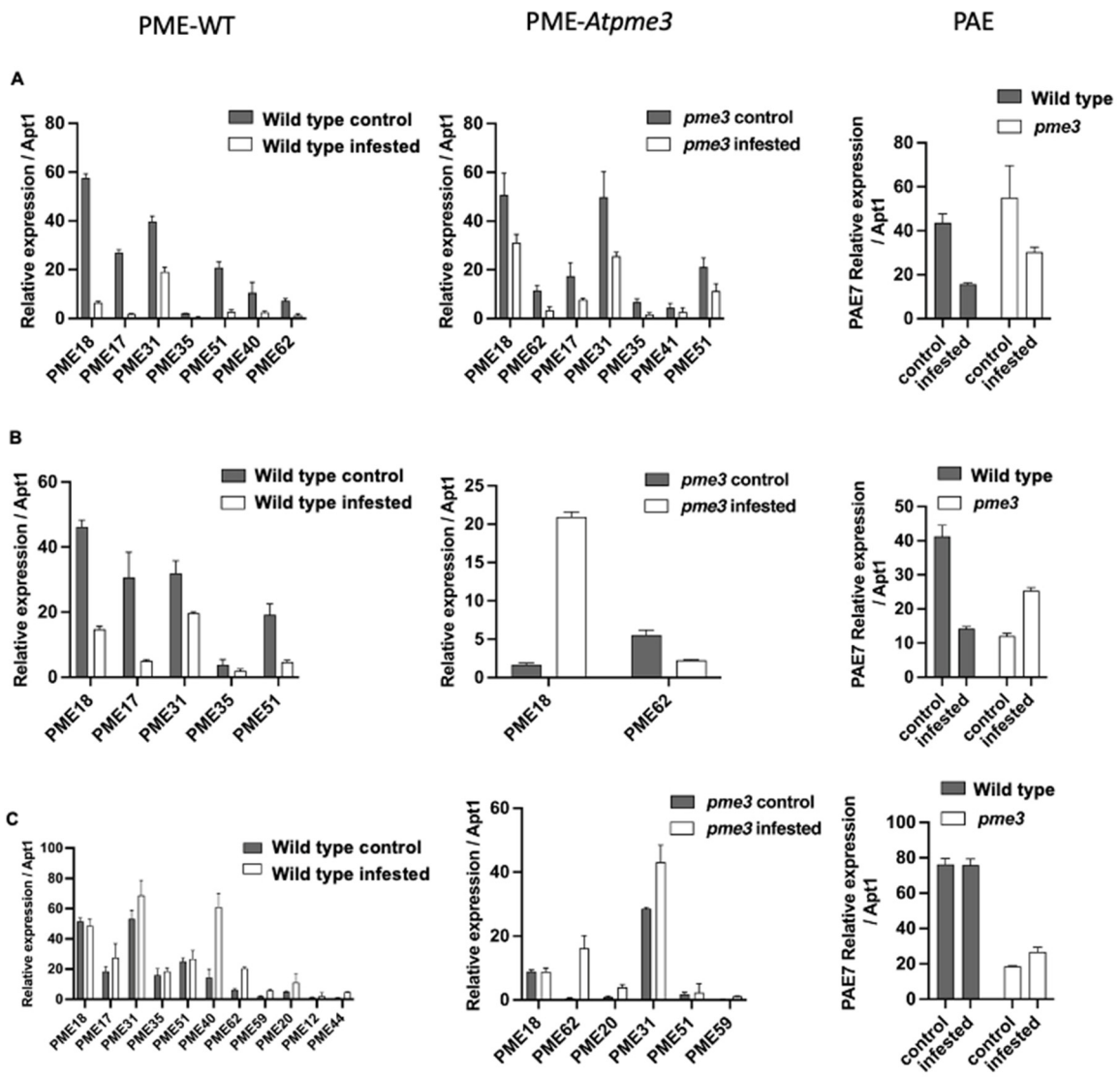

Figure 4. Expression patterns of PME and PAE gene families in roots of WT and *Atpme3-1* at pre-attachment (6 hai, 12 hai) and post attachment (8 dai, 14 dai) of *P. ramosa*. *Target genes were normalized to the housekeeping gene APT1 as internal control (n=2 technical replicates per genotype and condition).*

2.5. The Infestation Modulates PME and PAE Activities in WT and Atpme3-1 before and after Parasite Attachment

Because of the haustorium, it was impossible to isolate mechanically the parasitic tissues from the infected host roots. As mentionned above, WT and *Atpme3-1* roots were not infected before the second week of infestation. Thus, roots were free of parasite attachments at 6 hai, 12 hai and 8 dai. In contrast, host roots were infected at 14 dai by very young parasite attachments (stage 1 and 2), the number of which was however relatively low and the total weight was also extremely low in comparison with the host root weight. Then PME and PAE activities measured from infected roots at 14 dai could be considered belonging to the host (Figure 5).

At the early time point corresponding to 6 hai, WT and *Atpme3-1* in control conditions presented similar PAE activities, while *Atpme3*-1 differed from WT by lower PME activity (Figure 5B). Under infestation, PAE and PME activities significantly decreased in both genotypes, in accordance with the decrease in expression of *PAE7* and all the *PME* genes at this time point (Figure 4).

At the time point corresponding to 12 hai, PAE and PME activities in control conditions were significantly higher in WT than in *Atpme3-1* (Figure 5A,B). PAE activity in control WT increased when compared to 6 hai while PME activity did not change significantly. In contrast, control *Atpme3-1*

 doi:10.20944/preprints202407.1259.v1

exhibited a slight increase in PME activity at 12 hai. Under infestation, a slight decrease in PAE activity in WT but no significant change in *Atpme3-1* were observed. On the contrary, no change in PAE activity in addition to a significant decrease in PME3 activity occurred at 12 hai in *Atpme3-1* in response to infestation. In this way, infestation-induced changes in PAE activity and *PAE7* gene expression matched at 6 hai and 12 hai in WT, and only at 6 hai in *Atpme3-1* (Figure 4, A-PAE and Figure 5A). Moreover, this finding discordes with the decrease in PME activity in *Atpme3-1* at 12 hai (Figure 5, B-PME *Atpme3-1*).

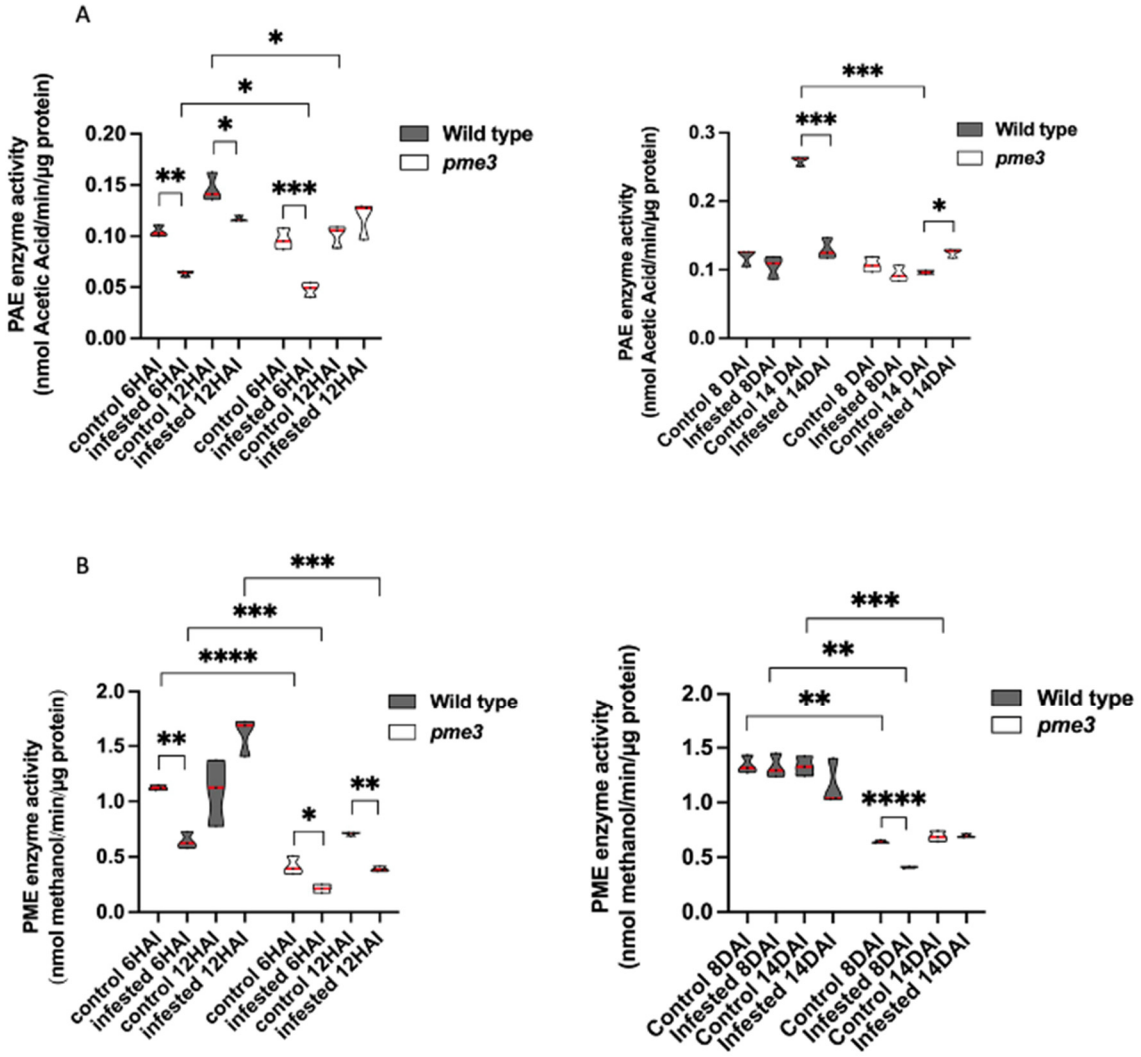

Figure 5. PRE enzymatic activities (PAE activity (A) and PME activity (B)) in roots of WT and Atpme3-1 at pre-attachment (6 hai, 12 hai) and post attachment (8 dai, 14 dai) of *P. ramosa*. Red line represents the median, black line the quartiles, (n=3 biological replicates per genotype). *, $P < 0.05$, **, $P < 0.001$, ***, $P < 0.0001$, T-Test.

Later, at 8 dai, the infestation did not impact PAE activity in both genotypes and PME activity in WT (Figure 5A,B). Only PME activity slightly decreased in *Atpme3-1* when infested.

At 14 dai, PME activity was not impacted by infestation in both genotypes (Figure 5B) whereas PAE activity strongly decreased in infected WT and slightly increased in infected *Atpme3-1* (Figure 5A,B).

Overall, PME activities were almost twice lower in *Atpme3-1* compared to WT under both control and infestation conditions and at all the time points (Figure 5B).

 doi:10.20944/preprints202407.1259.v1

3. Discussion

Pectins are major components of primary plant cell wall and ensure cohesion between cells [33]. Pectin remodeling occurs during plant growth and development by various PREs enzymes including PAE and PME [22]. Maintaining cell wall integrity is crucial in adaptation and establishment of tolerance mechanisms for stress, particularly biotic stress [6]. Mechanisms controlling this integrity need investigations, particularly in the context of the parasitic plant-plant interactions, for which information is scarce.

Guénin et al. (2011) carried out the first investigations on pectin remodeling in roots of the mutant *Atpme3-1*. In addition to a low HG content, the mutation induced a significant decrease in PME activity in accordance with a modified pectin pattern in favor of highly methylesterified HGs. Given that such changes normally limit the action of hydrolytic enzymes from pathogens [34–37], *Atpme3-1* is effectively less susceptible to pathogenic microorganisms and nematodes [11,27], revealing the contribution of AtPME3 in susceptibility to those pathogens. Moreover, in the interaction between *A. thaliana* and the nematode *Heterodera schachtii*, Hewezi et al. (2008) showed that AtPME3 binds to the effector, the Cellulose Binding Protein (CBP), leading to changes in host cell wall that facilitate infestation. The present study confirm limitation in PME activity in *Atpme3-1* roots (Figure 5B,C), but contrast by the fact that *Atpme3-1* turns out much more susceptible to the parasitic plant *P. ramosa* than WT (Figure 2) and that the parasite develops faster when attached to *Atpme3-1*. Thus, the findings show that pectin remodeling in *Atpme3-1* roots promotes successful in parasite attachment and in following tubercle development, and finally that changes in cell wall induced by *PME3* mutation affects negatively or positively the sensitivity to pathogens according to the infecting organism.

In the present study, immunohistochemical studies using LM19 and LM20 antibodies show high pectin DM of vascular cell walls in WT and *Atpme3-1* roots under control conditions (Figure 3A,B). According to Guénin et al. (2011), *Atpme3-1* displayed a DM of uronic acids 1.4 times higher compared with WT in 10 d-old roots and hypocotyls (FT-IR technology). Such difference could not be detected at tissue and cellular levels in the present study. On the other hand, the immunohistochemical studies on infected roots harvested early during infection (stage 1-attachments, 14 dai) emphasize the decrease in pectin DM at the host-parasite interface specifically in *Atpme3-1* in response to infection (Figure 3B,F) while infection did not induce changes in WT (Figure 3A,E). This finding suggests that enhanced susceptibility in *Atpme3-1* result from cell wall release at the host-parasite interface more conducive to haustorium development and parasite attachment. It thus reinforces the interest to assess PRE encoding gene expression and enzyme activities in WT and *Atpme3-1* roots during infestation.

Pectin esterases, including PAE and PME, are essential to pectin remodeling [38,39]. Vieira Dos Santos et al. (2003) reported that infestation induced general response signalling pathways involved in plant defence before parasite attachment to *A. thaliana* (WS) roots. Our results show that the host roots perceive the parasite early during infestation in both WT and *Atpme3-1*, resulting in a concomitant reduction in PAE and PME gene expression and activities at 6 hai, well before the parasite has penetrated the host roots. Among the PAE multigenic family, only *PAE7* expressed concomitantly in lower extent in both infested genotypes (Figure 4A,B). In addition, among the 66 PME-encoding genes, only 8 expressed in WT and *Atpme3-1* and also decreased early at 6 hai in response to infestation. Four of them (*PME 17, PME 18, PME 31* and *PME 35*) are strongly expressed in response to pathogens, in particular bacteria and nematodes [22,27,41,42]. Conversely, WT and *Atpme3-1* responded differently to infestation at 12 hai. For example, PME-encoding gene and *PAE7* expression were still affected by infestation in WT while *PME18* and *PAE7* overexpressed in *Atpme3-1* (Figure 4A,B). Changes in gene expression and enzyme activities did not match at this time point of infestation since PAE activity declined in WT but not in *Atpme3-1* whereas PME activity declined in *Atpme3-1* but not in WT (Figure 5A). Such mismatches were also found for PME at 14 dai and also in previous studies [43,44]. They address notably the question about the involvement of PMEI to regulate PME activity [45,46], notably given that five PME from WT and *Atpme3-1* display an N-terminal extension (PRO region) with similarities with the PMEI domain (Pfam04043, [47]. Later, once

 doi:10.20944/preprints202407.1259.v1

parasite attached (14 dai), enzyme activities tended to be less impacted in host roots, excepted in WT where PAE activity decreased strongly (Figure 5B). Randoux et al. (2010) proposed that the degree of pectin acetylation is a key point in the response of wheat to mildew since treatment with acetylated OGs prior to infection inhibited the growth of the pathogenic haustorium. Our finding then suggest that WT might retain a higher degree of pectin acetylation in roots, then limiting parasite attachment by preventing the action of potential parasite's PG, resulting in high susceptibility to *P. ramosa* in comparison to *Atpme3-1*.

Understanding the role of PRE in the parasitic plant-plant interaction is challenging by the fact that the infecting organism is also an angiosperm, which makes it more challenging for host plants to recognize it as a pathogen, ant that the plant cell wall may actually appear as the assembly of multiple specific cell wall microdomains. HGs vary in size with various degrees of polymerization and in charge [49]. Moreover, the multigenic families of PREs are similar in size (about 70 genes each in *Arabidopsis thaliana*, [50,51], rendering theoretically plausible the combinatory interactions of individual members. In addition, precise and dynamic modulation of extracellular pH controls HG-modifying enzyme activities, and in particular PME and PG [52]. Complete functional studies including host and parasite's PRE should be addressed in the future within the parasitic plant-plant interaction, particularly when it comes to understand the molecular interactions between various cell wall components.

4. Materials and Methods

4.1. Plant Material and Growth Conditions

Phelipanche ramosa (L.) Pomel (genetic type 1, lab reference: Pram10, [53]) seeds were collected in 2011 from mature broomrape flowering spikes in an oilseed rape field at Saint Martin de Fraigneau (France) and stored at 25 °C in the dark before use. *Arabidopsis thaliana* (L.) Heynh WS (Wassilewskija) wild type (WT) ecotype and WS *Atpme3-1* mutant ecotype (isolated from the Versailles T-DNA insertion collection (FLAG585E02)) were used for co-cultivation experiments in Petri dishes. Two hundred *Arabidopsis thaliana* seeds of each ecotype were surface-sterilized, by placing them in an Eppendorf tube containing ethanol 70 % (v:v) and SDS 0.05 % (v:v) up to 2 mL. The tube was placed on a stirring table during 5 min (70 rpm), and then the liquid was removed and replaced by ethanol 90 %. The tube was stirred 5 min again, the liquid removed and seeds put to dry overnight under a suction hood. Using a sterile toothpick, seeds were placed on square Petri dishes (12 cm x 12 cm) containing ½ MS MES medium and incubated at 21 °C in a growth chamber (16 h light, 120 µmoles PAR m^{-2} s^{-1}, 8 h dark) for 21 d.

4.2. Induction of Broomrape Seed Germination

P. ramosa seeds (200 mg) were surface-sterilized for 5 min with 12 % sodium hypochlorite in a 50 mL plastic tube, and thoroughly rinsed three times with sterile distilled water [54]. Seeds were then suspended (10 mg mL^{-1}) in 1 mM HEPES, pH 7.5, 0.1 % (w/v) PPM Plant Preservative Mixture and incubated for 7 d at 21 °C in the dark to be conditioned. Then germination was induced by adding *Rac*-GR24, a synthetic germination stimulant (final concentration: 10^{-9} M). Subsequently, seeds were incubated for 3 d at 21 °C in the dark for germination. Seeds, considered as germinated when the radicle protruded out of the seed coat, were used for plant infestations.

4.3. Co-Cultivation Experiments

Twenty-one day-old *A. thaliana* plantlets (WT or *Atpmei3-1*) were transferred onto filter paper and placed in cut square plates (120 × 120 × 17 mm, Greiner, France) containing a uniform layer of rockwool moisturized with 50 mL of ½ TT medium [55]. Each plate contained 5 plantlets. Plates were sealed and incubated vertically at 21 °C in a growth chamber (16 H light, 120 µmoles PAR m^{-2} s^{-1}, 8 h dark, 70 % humidity) for 7 d and supplied every 3 d with 10 mL of ½ TT medium. After 7 d, the infestation consisted in covering *A. thaliana* roots with 2 mL of germinated *P. ramosa* seeds (4000 germinated seeds per plate; germination rate: 86.03 ± 4.07 %). Previously, the seeds were rinsed three

 doi:10.20944/preprints202407.1259.v1

times with distilled water to remove any trace of GR24 and its solvent (0.2 % acetone) before being used. Plates were supplied every 3 d with 10 mL of ½ TT medium during 49 d. Controls consisted in non-infested plants.

Susceptibility to *P. ramosa* was assessed by counting the parasite attachments to the host roots under a stereo microscope (Olympus SZX10, Olympus Europa GmbH Hamburg, Germany). The counts were made at early time points (6 h after infestation (hai), 12 hai and later (8 days after infestation (8 dai), 14 dai, 28 dai and 42 dai), and by distinguishing 3 developmental stages (Figure 6). Each modality (control and infested WT and *Atpme3-1* plants) was performed using at least 5 plates, each plate containing 5 plants. Then data are means ± confident intervals (n≥25, multiple T-Test (FDR correction 0.1 %)).

The roots of control and infested plants were also collected at 6 hai, 12 hai, 8 dai and 14 dai, and immediately placed in liquid nitrogen for further molecular analyses and enzymatic assays.

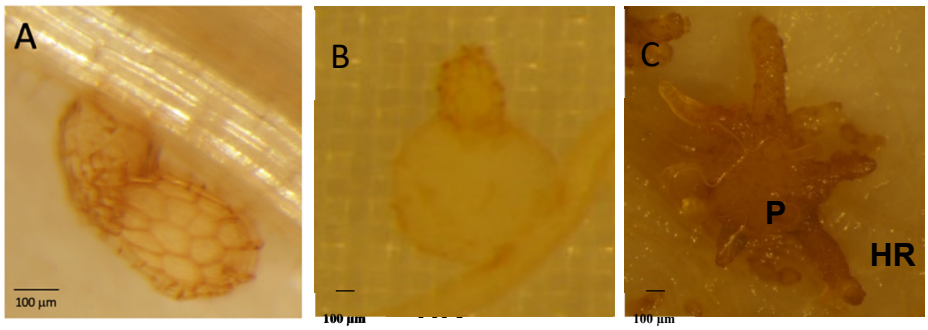

Figure 6. Different stages of *P. ramosa* for phenotyping the number of attachments on roots of *A. thaliana*. (A) Stage 1 or young haustorium, (B) Stage 2 or young turbercle, (C) Stage 3 or tubercle with adventive roots. HR: host root, P: parasite.

4.4. Bioinformatic Analyses

PRE families (PME, PAE, PMEi, PG and PL) are associated with specific Pfam domains (PME: PF1095, PMEi: PF04043, PAE:PF03283, PG: PF00295, PL:PF00544, https//www.uniprot.org). Using InterProScan software (https://www.ebi.ac.uk/InterProScan) and UniProt sequence data (https//www.uniprot.org), Pfam domains were investigated in PRE protein sequences and PRE gene sequences in *P. ramosa* obtained by *de novo* transcriptome assembly [56].

4.5. Cytological Analyses

Control and infected secondary lateral roots harvested at 14 dai were cut into 1 cm and 0.5 cm from each side of the parasite attachment (stage 1) area, respectively. Root segments were immediately fixed in 4 % (w/v) paraformaldehyde containing 0.1 M sodium phosphate buffer (pH 7.4) to which 1 % (w/v) sucrose and 0.05 % (v/v) tween 20 were added [57]. Samples were finally placed in the center of capsules and in a heat chamber for 24 h. Polymerized samples were cut using an ultramicrotome (Leica ultracut UCT) and 2 µm sections were collected on poly-L-lysine-treated well glass slides. Plates (n=5 per modality) were analyzed under bright-field optics with a light microscope (Eclipse 90i, Nikon) and a stereoscopic microscope (SteREO Discovery V20, CARL ZEISS, Germany) depending on the desired resolution.

Immunolabeling of homogalacturonans (HG) from the selected samples was realized according to Turbant et al. (2016), using the primary monoclonal antibodies LM19 and LM20, which stain low and high methylesterified HGs, respectively (PlantProbes, University of Leeds, Leeds, http//:www.plantprobes.net). In addition, calcofluor White was used to visualize the cell walls by staining both cellulose and β-1,4 glycans. Samples were imaged with a confocal laser microscope (LSM 780, Carl Zeiss). Images were acquired with a x40 HCX PL APO CS 1.25 NA oil objective with the following parameters: image dimension (512 x 512), scanning speed (400 Hz), line average of 8, pinhole (1 airy unit). Laser power and gain settings for each PMT (PhotoMultiplier Tubes) were

 doi:10.20944/preprints202407.1259.v1

slightly adjusted individually for each sample. Images were collected in 8-bits per pixel. All recordings were performed at room temperature (20-25 °C). Image processing was performed with Zen imaging software (Zeiss) and ImageJ (W. Rasband, National Institutes of Health).

4.6. Targeted Transcriptomic Analyses

Total RNA was extracted from 100 mg of control and infested roots (6 and 12 hai, 14 dai) ground with liquid nitrogen using Macherey-Nagel™ RNA Plant and Fungi NucleoSpin™ according to the manufacturer's recommendations. Genomic DNA was removed using Turbo DNA-free™ kit (Ambion), according to the manufacturer's protocol. cDNA synthesis was performed using 4 µg of RNA, 2.5 µM oligo $(dT)_{18}$ and the Transcriptor High Fidelity cDNA Synthesis Kit (ROCHE), using the manufacturer's protocol. RT-qPCR analyses were performed on 1/20 diluted cDNA. For real-time quantitative PCR, the LightCycler 480 SYBR Green I Master (Roche; catalog no. 04887352001) was used on 384-well plates in the LightCycler480 Real-Time PCR System (Roche). The crossing threshold values for each sample (the number of PCR cycles required for the accumulated fluorescence signal to cross a threshold above the background) were acquired with the LightCycler 480 software (Roche) using the second derivative maximum method. Primers used are specific to the host *A. thaliana* and are shown in the Supplemental Table S1. Stably expressed reference genes (*APT1, TIP41* and *CLATHRIN*) were selected using GeNorm software [59], and used as internal controls to calculate the relative expression of target genes according to [60]. *AtPME* and *AtPAE* gene expression were measured using stably expressed reference genes mentioned above, in two biological samples and two technical replicates per biological replicate. As the results from the two biological samples showed similar changes in gene expression during infection, only the results obtained from one of the two biological replicate and with *APT1* as internal *control*, are shown.

4.7. Global Enzyme Assays

Enriched weakly bound cell wall proteins (CWP) were extracted from roots (6 hai and 12 hai, 8 dai and 14 dai) according to Roig-Oliver et al. (2020) for PME and PAE enzyme assays. Briefly, 100 mg of frozen root powder were homogenized in 300 µL of 50 mM sodium phosphate buffer (pH=7.5) containing 2 M sodium chloride. The homogenate was incubated at 4 °C for 30 min under shaking. After centrifugation and supernatant recovery, a second extraction was carried out on the pellet in the same conditions. The supernatants were mixed and desalted using a citrate-phosphate buffer, pH 6.5 (McIlvaine's buffer) containing 100 mM sodium chloride. The proteins were quantified with bovine serum albumin as standard [62].

PME activity was measured from the enriched CWP extract according to Baldwin et al. (2014). The protein extract (5 µL) was incubated with 95 µL of 50 mM sodium phosphate buffer (pH 7.5) containing 0.025 U alcohol oxidase (A2404, Sigma-Aldrich, St. Louis, MO, USA) and 100 µg 90 % methylesterified citrus pectin (P9561, Sigma-Aldrich, St. Louis, MO, USA). After 30 min of incubation at 28 °C, 100 µL of staining solution containing 20 mM pentane-2,4-dione and 50 mM glacial acetic acid in a 2 M ammonium acetate buffer were added. Absorbance at 420 nm was measured in a microplate reader (Powerwave, Biotek, Colmar, France) after a 15 min incubation at 68 °C. PME activity was determined with reference to a methanol standard curve and expressed in nmol of methanol min^{-1} $µg^{-1}$ protein.

PAE activity was measured from the enriched CWP extract using triacetin (525073, Sigma-Aldrich, St. Louis, MO, USA) and sugar beet pectin (42 % methylesterification and 31 % acetylation degrees, CP Kelco) as substrate, respectively. Triacetin 100 mM was prepared in McIlvaine's buffer (pH 6.5) containing 100 mM sodium chloride. Sugar beet pectin (10 mg) was suspended in 1 mL of the same buffer. Activity was measured with 130 µL of substrate and 20 µg of CWP extract in a final volume of 150 µL incubated at 40 °C for 2h. The amount of released acetic acid was determined using the Megazyme acetic acid kit (Megazyme, K-ACETRM) at 340 nm using a microplate reader (BioTek PowerWave). Data are mean ± confident intervals (n = 3 biological replicates, T-Test).

 doi:10.20944/preprints202407.1259.v1

Author Contributions: CG, CV, PS, PD, SB and KP designed the experimental work. CG, CV, CG, YM, LM, FF, JD, PM, LZ, PS, SB, and KP implemented the experiments, collected and analyzed the data. CG, CV, CR, PS, SB and KP wrote the manuscript, all authors read and edited the manuscript. All authors have agreed to the published version of the manuscript.

Funding: This research received no funding.

Acknowledgments: We thank the CRRBM (Centres de Ressources Régionales en Biologie Moléculaire, Amiens, France) for the use of the molecular platform and the realization of real-time quantitative PCR analyses.

Conflicts of Interest: The authors declare that the research was conducted in the absence of any commercial or financial relationships that could be construed as a potential conflict of interest.

References

1. Fernández-Aparicio, M.; Reboud, X.; Gibot-Leclerc, S. Broomrape weeds. Underground mechanisms of parasitism and associated strategies for their control: A review. *Front. Plant Sci.* **2016**, *7*, doi:10.3389/fpls.2016.00135.
2. Cartry, D.; Steinberg, C.; Gibot-Leclerc, S. Main drivers of broomrape regulation. A review. *Agron. Sustain. Dev.* **2021**, *41*, doi:10.1007/s13593-021-00669-0.
3. Goyet, V.; Wada, S.; Cui, S.; Wakatake, T.; Shirasu, K.; Montiel, G.; Simier, P.; Yoshida, S. Haustorium Inducing Factors for Parasitic Orobanchaceae. *Front. Plant Sci.* **2019**, *10*, 1–8, doi:10.3389/fpls.2019.01056.
4. Brun, G.; Spallek, T.; Simier, P.; Delavault, P. Molecular actors of seed germination and haustoriogenesis in parasitic weeds. *Plant Physiol.* **2021**, *185*, 1270–1281, doi:10.1093/plphys/kiaa041.
5. Jhu, M.Y.; Sinha, N.R. Parasitic Plants: An Overview of Mechanisms by Which Plants Perceive and Respond to Parasites. *Annu. Rev. Plant Biol.* **2022**, *73*, 433–455, doi:10.1146/annurev-arplant-102820-100635.
6. Le Gall, H.; Philippe, F.; Domon, J.M.; Gillet, F.; Pelloux, J.; Rayon, C. Cell wall metabolism in response to abiotic stress. *Plants* **2015**, *4*, 112–166, doi:10.3390/plants4010112.
7. Carpita, N.C.; Gibeaut, D.M. Structural models of primary cell walls in flowering plants: Consistency of molecular structure with the physical properties of the walls during growth. *Plant J.* **1993**, *3*, 1–30, doi:10.1111/j.1365-313X.1993.tb00007.x.
8. McCann, M.C.; Roberts, K. Architecture of the primary cell wall. In *The Cytoskeletal Basis of Plant Growth and Form*; Lloyd, C.W., Ed.; Academic Press, 1991; pp. 109–129.
9. Jarvis, M.C.; Briggs, S.P.H.; Knox, J.P. Intercellular adhesion and cell separation in plants. *Plant, Cell Environ.* **2003**, *26*, 977–989, doi:10.1046/j.1365-3040.2003.01034.x.
10. Kämper, J.; Kahmann, R.; Bölker, M.; Ma, L.J.; Brefort, T.; Saville, B.J.; Banuett, F.; Kronstad, J.W.; Gold, S.E.; Müller, O.; et al. Insights from the genome of the biotrophic fungal plant pathogen Ustilago maydis. *Nature* **2006**, *444*, 97–101, doi:10.1038/nature05248.
11. Mitsumasu, K.; Seto, Y.; Yoshida, S. Apoplastic interactions between plants and plant root intruders. *Front. Plant Sci.* **2015**, *6*, 1–17, doi:10.3389/fpls.2015.00617.
12. Singh, A.; Singh, M. Cell wall degrading enzymes in Orobanche aegyptiaca and its host Brassica campestris. *Physiol. Plant.* **1993**, *89*, 177–181, doi:10.1111/j.1399-3054.1993.tb01802.x.
13. Véronési, C.; Bonnin, E.; Benharrat, H.; Fer, A.; Thalouarn, P. Opinion: Are pectinolytic activities of Orobanche cumana seedlings related to virulence towards sunflower? *Isr. J. Plant Sci.* **2005**, *53*, 19–27, doi:10.1560/ETEL-C34X-Y6MG-YT0M.
14. González-Verdejo, C.I.; Barandiaran, X.; Moreno, M.T.; Cubero, J.I.; Di Pietro, A. A peroxidase gene expressed during early developmental stages of the parasitic plant Orobanche ramosa. *J. Exp. Bot.* **2006**, *57*, 185–192, doi:10.1093/jxb/erj024.
15. Honaas, L.A.; Wafula, E.K.; Yang, Z.; Der, J.P.; Wickett, N.J.; Altman, N.S.; Taylor, C.G.; Yoder, J.I.; Timko, M.P.; Westwood, J.H.; et al. Functional genomics of a generalist parasitic plant: Laser microdissection of host-parasite interface reveals host-specific patterns of parasite gene expression. *BMC Plant Biol.* **2013**, *13*, doi:10.1186/1471-2229-13-9.
16. Yang, Z.; Wafula, E.K.; Honaas, L.A.; Zhang, H.; Das, M.; Fernandez-Aparicio, M.; Huang, K.; Bandaranayake, P.C.G.; Wu, B.; Der, J.P.; et al. Comparative transcriptome analyses reveal core parasitism genes and suggest gene duplication and repurposing as sources of structural novelty. *Mol. Biol. Evol.* **2015**, *32*, 767–790, doi:10.1093/molbev/msu343.
17. Losner-Goshen, D.; Portnoy, V.H.; Mayer, A.M.; Joel, D.M. Pectolytic activity by the haustorium of the parasitic plant Orobanche L. (Orobanchaceae) in host roots. *Ann. Bot.* **1998**, *81*, 319–326, doi:10.1006/anbo.1997.0563.
18. Johnsen, H.R.; Striberny, B.; Olsen, S.; Vidal-Melgosa, S.; Fangel, J.U.; Willats, W.G.T.; Rose, J.K.C.; Krause, K. Cell wall composition profiling of parasitic giant dodder (Cuscuta reflexa) and its hosts: A priori differences and induced changes. *New Phytol.* **2015**, *207*, 805–816, doi:10.1111/nph.13378.

19. Hématy, K.; Cherk, C.; Somerville, S. Host-pathogen warfare at the plant cell wall. *Curr. Opin. Plant Biol.* **2009**, *12*, 406–413, doi:10.1016/j.pbi.2009.06.007.
20. Ferrari, S.; Savatin, D. V.; Sicilia, F.; Gramegna, G.; Cervone, F.; De Lorenzo, G. Oligogalacturonides: Plant damage-associated molecular patterns and regulators of growth and development. *Front. Plant Sci.* **2013**, *4*, 1–9, doi:10.3389/fpls.2013.00049.
21. Shibuya, N.; Minami, E. Oligosaccharide signalling for defence responses in plant. *Physiol. Mol. Plant Pathol.* **2001**, *59*, 223–233, doi:10.1006/pmpp.2001.0364.
22. Sénéchal, F.; Graff, L.; Surcouf, O.; Marcelo, P.; Rayon, C.; Bouton, S.; Mareck, A.; Mouille, G.; Stintzi, A.; Höfte, H.; et al. Arabidopsis PECTIN METHYLESTERASE17 is co-expressed with and processed by SBT3.5, a subtilisin-like serine protease. *Ann. Bot.* **2014**, *114*, 1161–1175, doi:10.1093/aob/mcu035.
23. Kohorn, B.D.; Kohorn, S.L.; Saba, N.J.; Martinez, V.M. Requirement for pectin methyl esterase and preference for fragmented over native pectins for wall-associated kinase-activated, EDS1/PAD4-dependent stress response in arabidopsis. *J. Biol. Chem.* **2014**, *289*, 18978–18986, doi:10.1074/jbc.M114.567545.
24. Brutus, A.; Sicilia, F.; Macone, A.; Cervone, F.; De Lorenzo, G. A domain swap approach reveals a role of the plant wall-associated kinase 1 (WAK1) as a receptor of oligogalacturonides. *Proc. Natl. Acad. Sci. U. S. A.* **2010**, *107*, 9452–9457, doi:10.1073/pnas.1000675107.
25. Lejeune, A.; Constant, S.; Delavault, P.; Simier, P.; Thalouarn, P.; Thoiron, S. Involvement of a putative Lycopersicon esculentum wall-associated kinase in the early steps of tomato-Orobanche ramosa interaction. *Physiol. Mol. Plant Pathol.* **2006**, *69*, 3–12, doi:10.1016/j.pmpp.2006.12.001.
26. Hewezi, T.; Howe, P.; Maier, T.R.; Hussey, R.S.; Mitchum, M.G.; Davis, E.L.; Baum, T.J. Cellulose binding protein from the parasitic nematode heterodera Schachtii interacts with arabidopsis pectin methylesterase: Cooperative cell wall modification during parasitism. *Plant Cell* **2008**, *20*, 3080–3093, doi:10.1105/tpc.108.063065.
27. Raiola, A.; Lionetti, V.; Elmaghraby, I.; Immerzeel, P.; Mellerowicz, E.J.; Salvi, G.; Cervone, F.; Bellincampi, D. Pectin methylesterase is induced in Arabidopsis upon infection and is necessary for a successful colonization by necrotrophic pathogens. *Mol. Plant-Microbe Interact.* **2011**, *24*, 432–440, doi:10.1094/MPMI-07-10-0157.
28. Guénin, S.; Mareck, A.; Rayon, C.; Lamour, R.; Assoumou Ndong, Y.; Domon, J.M.; Sénéchal, F.; Fournet, F.; Jamet, E.; Canut, H.; et al. Identification of pectin methylesterase 3 as a basic pectin methylesterase isoform involved in adventitious rooting in Arabidopsis thaliana. *New Phytol.* **2011**, *192*, 114–126, doi:10.1111/j.1469-8137.2011.03797.x.
29. Pérez-De-Luque, A.; Lozano, M.D.; Cubero, J.I.; González-Melendi, P.; Risueño, M.C.; Rubiales, D. Mucilage production during the incompatible interaction between Orobanche crenata and Vicia sativa. *J. Exp. Bot.* **2006**, *57*, 931–942, doi:10.1093/jxb/erj078.
30. Pelloux, J.; Rustérucci, C.; Mellerowicz, E.J. New insights into pectin methylesterase structure and function. *Trends Plant Sci.* **2007**, *12*, 267–277, doi:10.1016/j.tplants.2007.04.001.
31. Roig-Oliver, M.; Fullana-Pericàs, M.; Bota, J.; Flexas, J. Adjustments in photosynthesis and leaf water relations are related to changes in cell wall composition in Hordeum vulgare and Triticum aestivum subjected to water deficit stress. *Plant Sci.* **2021**, *311*, doi:10.1016/j.plantsci.2021.111015.
32. Olsen, S.; Striberny, B.; Hollmann, J.; Schwacke, R.; Popper, Z.; Krause, K. Getting ready for host invasion: Elevated expression and action of xyloglucan endotransglucosylases/hydrolases in developing haustoria of the holoparasitic angiosperm Cuscuta. *J. Exp. Bot.* **2016**, *67*, 695–708, doi:10.1093/jxb/erv482.
33. Mohnen, D. Pectin structure and biosynthesis. *Curr. Opin. Plant Biol.* **2008**, *11*, 266–277, doi:10.1016/j.pbi.2008.03.006.
34. Boudart, G.; Lafitte, C.; Barthe, J.P.; Frasez, D.; Esquerré-tugayé, T.; Boudart, G.; Lafitte, C.; Barthe, J.P.; Frasez, D. Linked references are available on JSTOR for this article : Planta Differential elicitation of defense responses by pectic fragm in bean seedlings. **2024**, *206*, 86–94.
35. Limberg, G.; Körner, R.; Buchholt, H.C.; Christensen, T.M.I.E.; Roepstorff, P.; Mikkelsen, J.D. Analysis of different de-esterification mechanisms for pectin by enzymatic fingerprinting using endopectin lyase and endopolygalacturonase II from A. Niger. *Carbohydr. Res.* **2000**, *327*, 293–307, doi:10.1016/S0008-6215(00)00067-7.
36. Van Kan, J.A.L. Licensed to kill: the lifestyle of a necrotrophic plant pathogen. *Trends Plant Sci.* **2006**, *11*, 247–253, doi:10.1016/j.tplants.2006.03.005.
37. Lionetti, V.; Raiola, A.; Camardella, L.; Giovane, A.; Obel, N.; Pauly, M.; Favaron, F.; Cervone, F.; Bellincampi, D. Overexpression of pectin methylesterase inhibitors in Arabidopsis restricts fungal infection by Botrytis cinerea. *Plant Physiol.* **2007**, *143*, 1871–1880, doi:10.1104/pp.106.090803.
38. Manmohit Kalia, P.K. Pectin Methylesterases: A Review. *J. Bioprocess. Biotech.* **2015**, *05*, doi:10.4172/2155-9821.1000227.
39. Coculo, D.; Lionetti, V. The Plant Invertase/Pectin Methylesterase Inhibitor Superfamily. *Front. Plant Sci.* **2022**, *13*, doi:10.3389/fpls.2022.863892.

 doi:10.20944/preprints202407.1259.v1

40. Vieira Dos Santos, C.; Letousey, P.; Delavault, P.; Thalouarn, P. Defense gene expression analysis of Arabidopsis thaliana parasitized by Orobanche ramosa. *Phytopathology* **2003**, *93*, 451–457, doi:10.1094/phyto.2003.93.4.451.
41. Barcala, M.; García, A.; Cabrera, J.; Casson, S.; Lindsey, K.; Favery, B.; García-Casado, G.; Solano, R.; Fenoll, C.; Escobar, C. Early transcriptomic events in microdissected Arabidopsis nematode-induced giant cells. *Plant J.* **2010**, *61*, 698–712, doi:10.1111/j.1365-313X.2009.04098.x.
42. Bethke, G.; Grundman, R.E.; Sreekanta, S.; Truman, W.; Katagiri, F.; Glazebrook, J. Arabidopsis PECTIN METHYLESTERASEs contribute to immunity against Pseudomonas syringae. *Plant Physiol.* **2014**, *164*, 1093–1107, doi:10.1104/pp.113.227637.
43. Jamet, E.; Roujol, D.; San-Clemente, H.; Irshad, M.; Soubigou-Taconnat, L.; Renou, J.P.; Pont-Lezica, R. Cell wall biogenesis of Arabidopsis thaliana elongating cells: Transcriptomics complements proteomics. *BMC Genomics* **2009**, *10*, 505, doi:10.1186/1471-2164-10-505.
44. Minic, Z.; Jamet, E.; San-Clemente, H.; Pelletier, S.; Renou, J.P.; Rihouey, C.; Okinyo, D.P.; Proux, C.; Lerouge, P.; Jouanin, L. Transcriptomic analysis of arabidopsis developing stems: A close-up on cell wall genes. *BMC Plant Biol.* **2009**, *9*, 1–17, doi:10.1186/1471-2229-9-6.
45. Lionetti, V.; Raiola, A.; Cervone, F.; Bellincampi, D. Transgenic expression of pectin methylesterase inhibitors limits tobamovirus spread in tobacco and arabidopsis. *Mol. Plant Pathol.* **2014**, *15*, 265–274, doi:10.1111/mpp.12090.
46. Lionetti, V.; Fabri, E.; De Caroli, M.; Hansen, A.R.; Willats, W.G.T.; Piro, G.; Bellincampi, D. Three pectin methylesterase inhibitors protect cell wall integrity for arabidopsis immunity to Botrytis. *Plant Physiol.* **2017**, *173*, 1844–1863, doi:10.1104/pp.16.01185.
47. Louvet, R.; Cavel, E.; Gutierrez, L.; Guénin, S.; Roger, D.; Gillet, F.; Guerineau, F.; Pelloux, J. Comprehensive expression profiling of the pectin methylesterase gene family during silique development in Arabidopsis thaliana. *Planta* **2006**, *224*, 782–791, doi:10.1007/s00425-006-0261-9.
48. Randoux, B.; Renard-Merlier, D.; Mulard, G.; Rossard, S.; Duyme, F.; Sanssené, J.; Courtois, J.; Durand, R.; Reignault, P. Distinct defenses induced in wheat against powdery mildew by acetylated and nonacetylated oligogalacturonides. *Phytopathology* **2010**, *100*, 1352–1363, doi:10.1094/PHYTO-03-10-0086.
49. Bonnin, E.; Garnier, C.; Ralet, M.C. Pectin-modifying enzymes and pectin-derived materials: Applications and impacts. *Appl. Microbiol. Biotechnol.* **2014**, *98*, 519–532, doi:10.1007/s00253-013-5388-6.
50. Francoz, E.; Ranocha, P.; Burlat, V.; Dunand, C. Arabidopsis seed mucilage secretory cells: Regulation and dynamics. *Trends Plant Sci.* **2015**, *20*, 515–524, doi:10.1016/j.tplants.2015.04.008.
51. Scheler, C.; Weitbrecht, K.; Pearce, S.P.; Hampstead, A.; Büttner-Mainik, A.; Lee, K.J.D.; Voegele, A.; Oracz, K.; Dekkers, B.J.W.; Wang, X.; et al. Promotion of testa rupture during garden cress germination involves seed compartment-specific expression and activity of pectin methylesterases. *Plant Physiol.* **2015**, *167*, 200–215, doi:10.1104/pp.114.247429.
52. Hocq, L.; Pelloux, J.; Lefebvre, V. Connecting Homogalacturonan-Type Pectin Remodeling to Acid Growth. *Trends Plant Sci.* **2017**, *22*, 20–29, doi:10.1016/j.tplants.2016.10.009.
53. Stojanova, B.; Delourme, R.; Duffé, P.; Delavault, P.; Simier, P. Genetic differentiation and host preference reveal non-exclusive host races in the generalist parasitic weed Phelipanche ramosa. *Weed Res.* **2019**, *59*, 107–118, doi:10.1111/wre.12353.
54. Lechat, M.-M.; Pouvreau, J.-B.; Péron, T.; Gauthier, M.; Montiel, G.; Véronési, C.; Todoroki, Y.; Le Bizec, B.; Monteau, F.; Macherel, D.; et al. PrCYP707A1, an ABA catabolic gene, is a key component of Phelipanche ramosa seed germination in response to the strigolactone analogue GR24. *J. Exp. Bot.* **2012**, *63*, 5311–5322, doi:10.1093/jxb/ers189.
55. Tadano, T.; Tanaka, A. The effect of low phosphate concentrations in culture medium on early growth of several crop plants. *Japanese J. Soil Sci. Plant Nutr.* **1980**, *51*, 399–404.
56. Goyet, V.; Billard, E.; Pouvreau, J.B.; Lechat, M.M.; Pelletier, S.; Bahut, M.; Monteau, F.; Spíchal, L.; Delavault, P.; Montiel, G.; et al. Haustorium initiation in the obligate parasitic plant Phelipanche ramosa involves a host-exudated cytokinin signal. *J. Exp. Bot.* **2017**, *68*, 5539–5552, doi:10.1093/jxb/erx359.
57. Miart, F.; Fournet, F.; Dubrulle, N.; Petit, E.; Demailly, H.; Dupont, L.; Zabijak, L.; Marcelo, P.; Boudaoud, A.; Pineau, C.; et al. Cytological Approaches Combined With Chemical Analysis Reveals the Layered Nature of Flax Mucilage. *Front. Plant Sci.* **2019**, *10*, 684, doi:10.3389/fpls.2019.00684.
58. Turbant, A.; Fournet, F.; Lequart, M.; Zabijak, L.; Pageau, K.; Bouton, S.; Van Wuytswinkel, O. PME58 plays a role in pectin distribution during seed coat mucilage extrusion through homogalacturonan modification. *J. Exp. Bot.* **2016**, *67*, 2177–2190, doi:10.1093/jxb/erw025.
59. Vandesompele, J.; De Preter, K.; Pattyn, F.; Poppe, B.; Van Roy, N.; De Paepe, A.; Speleman, F. Accurate normalization of real-time quantitative RT-PCR data by geometric averaging of multiple internal control genes. *Genome Biol.* **2002**, *3*, doi:10.1186/gb-2002-3-7-research0034.
60. Gutierrez, L.; Mauriat, M.; Pelloux, J.; Bellini, C.; Van Wuytswinkel, O. Towards a systematic validation of references in real-time RT-PCR. *Plant Cell* **2008**, *20*, 1734–1735, doi:10.1105/tpc.108.059774.

 doi:10.20944/preprints202407.1259.v1

61. Roig-Oliver, M.; Rayon, C.; Roulard, R.; Fournet, F.; Bota, J.; Flexas, J. Reduced photosynthesis in Arabidopsis thaliana atpme17.2 and atpae11.1 mutants is associated to altered cell wall composition. *Physiol. Plant.* **2020**, *172*, 1439–1451, doi:10.1111/ppl.13186.
62. Bradford, M.M. A rapid and sensitive method for the quantitation of microgram quantities of protein utilizing the principle of protein-dye binding. *Anal. Biochem.* **1976**, *72*, 248–254, doi:10.1016/0003-2697(76)90527-3.
63. Baldwin, L.; Domon, J.M.; Klimek, J.F.; Fournet, F.; Sellier, H.; Gillet, F.; Pelloux, J.; Lejeune-Hénaut, I.; Carpita, N.C.; Rayon, C. Structural alteration of cell wall pectins accompanies pea development in response to cold. *Phytochemistry* **2014**, *104*, 37–47, doi:10.1016/j.phytochem.2014.04.011.